Separation Science and Technology
Publication details, including instructions for authors and subscription information:
http://www.informaworld.com/smpp/title~content=t713708471

Gel Permeation Chromatography Using a Bio-Glas Substrate Having a Broad Pore Size Distribution

A. R. Cooper[a]; J. H. Cain[a]; E. M. Barrall Ii[ab]; J. F. Johnson[ac]
[a] CHEVRON RESEARCH COMPANY RICHMOND, CALIFORNIA [b] IBM Research Laboratory. San Jose, California [c] Department of Chemistry, and Institute of Materials Science, University of Connecticut, Storrs, Connecticut

To cite this Article Cooper, A. R. , Cain, J. H. , Barrall Ii, E. M. and Johnson, J. F.(1970) 'Gel Permeation Chromatography Using a Bio-Glas Substrate Having a Broad Pore Size Distribution', Separation Science and Technology, 5: 6, 787 — 800
To link to this Article: DOI: 10.1080/00372367008055540
URL: http://dx.doi.org/10.1080/00372367008055540

SEPARATION SCIENCE, 5(6), pp. 787–800, December, 1970

Gel Permeation Chromatography Using a Bio-Glas* Substrate Having a Broad Pore Size Distribution†

A. R. COOPER, J. H. CAIN, E. M. BARRALL II,‡
and J. F. JOHNSON§
CHEVRON RESEARCH COMPANY
RICHMOND, CALIFORNIA 94802

Summary

Gel permeation chromatography has been performed using a porous glass of broad pore size distribution, which was subjected to hexamethyldisilazane treatment. The elution volumes and peak widths of narrow molecular weight distribution polystyrenes using toluene as solvent have been determined. The physical characteristics of the porous glass have been studied by the methods of mercury porosimetry, nitrogen adsorption-desorption isotherms, and electron microscopy. The characteristics of this column packing material are compared with other packing materials in popular use.

INTRODUCTION

Recently a porous glass having a wide range of pore sizes, of suitable dimensions for the separation of high molecular weight polymers, became available to us (Bio-Glas BRX 85001, Bio-Rad Laboratories Richmond, Cal.). The elution volume–molecular weight relationship and the widths of the eluted peaks have not previously been obtained on a porous glass column with such a broad pore size distribution.

* Trademark name of a porous glass packing sold by Bio-Rad Laboratories, Richmond, California.

† Presented at the ACS Symposium on Gel Permeation Chromatography, sponsored by the Division of Petroleum Chemistry at the 159th National Meeting of the American Chemical Society, Houston, Texas, February, 1970.

‡ Present address: IBM Research Laboratory, San Jose, California 95114.

§ Present address: Department of Chemistry and Institute of Materials Science, University of Connecticut, Storrs, Connecticut 06268.

Thus, it became important to compare the gel permeation chromatography (GPC) characteristics of this packing with other available column packings to gain further insight into the mechanism of GPC. The porous glasses currently in use for GPC have either an intermediate pore size distribution (*1–3*) or an extremely uniform pore size (*4, 5*). Polystyrene gels have been shown by electron microscopy to have a very broad pore size distribution and, in general, have higher efficiencies than the porous glass columns (*6*). Porous silica beads which have recently been studied as a column packing have a distribution of pore sizes similar to the intermediate pore size distribution porous glasses.

EXPERIMENTAL

The glass as received contained a large distribution of particle sizes. For this study the 100–200 mesh fraction was separated using Tyler sieves and accounted for ~25% of the total weight. This fraction, after pretreatment under vacuum at 400°F for 2 hr, was treated with hexamethyldisilazane by refluxing in *n*-hexane for 6 hr. The water flotation test showed complete reaction with the surface hydroxyl groups. This was found to be a more convenient procedure than the vapor phase method (*7*). A column 64.5 in. long of ⅜-in. o.d. stainless steel tubing was packed dry and then pumped with solvent for 48 hr. Polystyrene fractions of narrow molecular weight distribution (MWD) were eluted from this column using toluene as solvent at room temperature using a chromatograph with a differential refractometer detector. Samples as 0.1% solutions were injected by displacement from a loop having a volume of 1.77 ml. Flow rates were 1.05 and 0.4 ml/min.

The siphon used for flow rate measurement was made according to the design of Gray (*8*) Type B nominal 5 ml which gives a volume dump of excellent constancy. This new siphon was calibrated for each flow rate used. The siphon chamber was saturated with solvent to eliminate evaporation errors (*9*).

Mercury porosimetry and nitrogen adsorption–desorption isotherm characterizations were carried out on samples that had been pretreated under vacuum for 2 hr at 400°F.

ELECTRON MICROSCOPY

A well-mixed 0.3 g portion of the crushed glass having particle sizes 100–200 mesh was mixed with an epoxy mounting resin prepolymer as

described previously (*3*). The impregnated samples were cast into the shape required by the Ultratome II ultramicrotome. Numerous sections were cut and floated onto carbon-coated electron microscope grids. Those sections thinner than 1000 Å (by interference color) were chosen for observation. The samples and grids were coated with carbon in a vacuum sputtering apparatus.

No replication or shadowing was required as the electron contrast between the glass and the resin mounting was satisfactory for direct observation. The carbon coating was required to avoid the beam-induced sample charge. A Japan Electron Optics JEM 6-A electron microscope operated at 80 kV was used to examine the samples. The micrographs were made on Kodak medium projector slide glass plates developed in Kodak HRP high resolution developer. The magnification of the microscope at 80 kV was calibrated by the standard diffraction grating technique.

RESULTS

Physical Characterization

Table 1 lists the physical characteristics of the porous glass, which had been treated with hexamethyldisilazane, determined by mercury intrusion and nitrogen adsorption techniques. The calculations of pore radius are based on a cylindrical pore model. The cumulative pore volume and differential pore volume plots with respect to the logarithm of the pore radius are shown in Fig. 1.

The nitrogen desorption isotherm showed that there was very little pore volume of pore radius less than 21 Å. In Fig. 1 the differential pore volume distribution shows that there are some very large pores in this

TABLE 1

Mercury porosimetry Contact angle 140° Surface tension, 473 dynes/cm	Pore volume, cc/g, 21.1 → 67,000 Å pore radius	0.47
	Macro pore volume, cc/g, 500 → 67,000 Å pore radius	0.21
	Micro pore volume, cc/g, 21.1 → 500 Å pore radius	0.26
Nitrogen adsorption–desorption Isotherms	BET surface area, m^2/g	48.3
	Liquid nitrogen micropore volume, cc/g, <500 Å pore radius	0.26

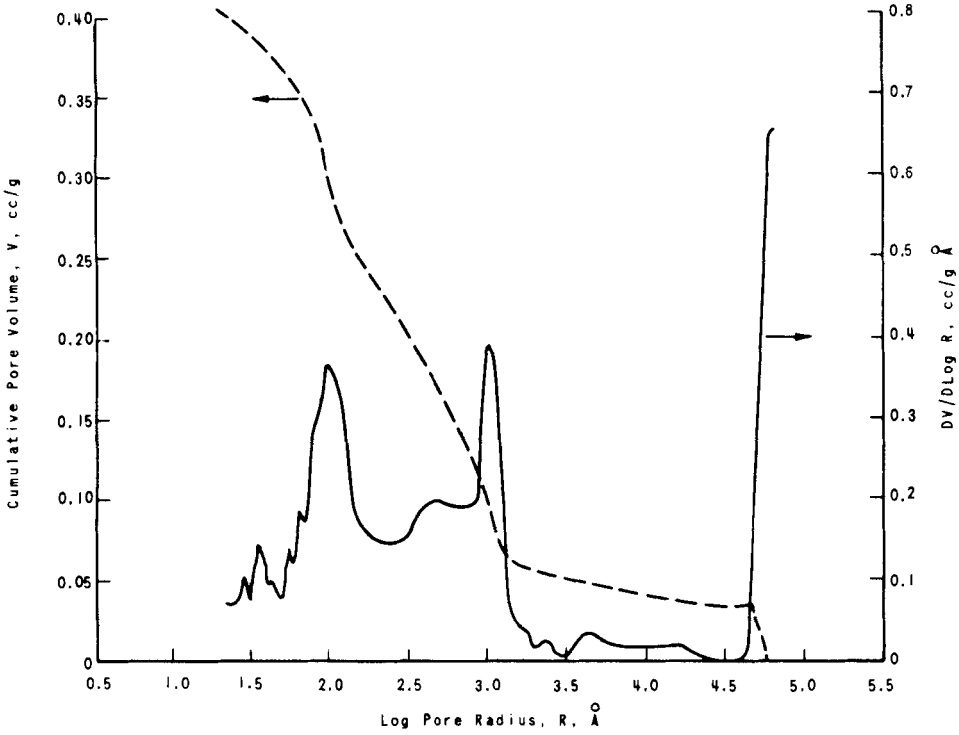

FIG. 1. Characterization of porous glass broad pore size distribution 100–200 mesh, disilazaned, by mercury porosimetry.

material. The peak at log $R = 4.8$ probably represents the filling of the interstitial voids in the bed of particles in the porosimeter cell. The mercury penetration data show that there are pores present in the material with radii of 17,800 Å. There is virtually a continuous distribution of pore radii down to the lower limit ~25 Å of the porosimeter instrument. Two peaks on the differential pore volume distribution plot, corresponding to pore radii of 100 and 1000 Å, contribute the major portion of the total pore volume.

The gross optical appearance of the chips was the same as that seen previously for the narrower pore size distribution samples. The chips were obviously made by crushing a larger lump of glass. Figures 2–4 summarize the appearance of the thin sections in the electron microscope. The figures are positive prints taken from the glass negatives.

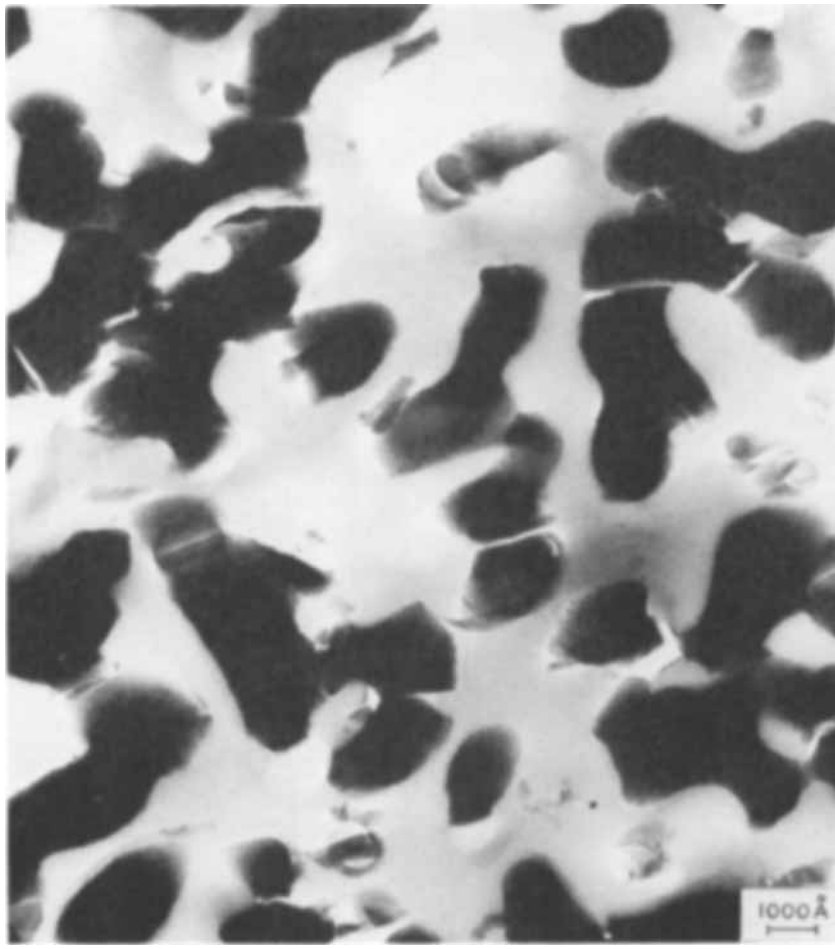

FIG. 2. Electron micrograph of broad pore diameter distribution Bio-Glas. Magnification of 100,000 diameters, sample mounted in epoxy resin with carbon coating. No metal shadowing. Positive print of glass negative. Dark areas represent glass walls.

The dark areas in the prints are the glass walls of the pores. The gray areas are the epoxy mounting resin. A few open areas exist where the resin did not penetrate or large glass walls dropped out. All channels appear to interconnect. The magnification of 100,000 diameters was verified with a diatom sample. Some optical gradation is noted where two layers of glass wall overlap due to sample thickness.

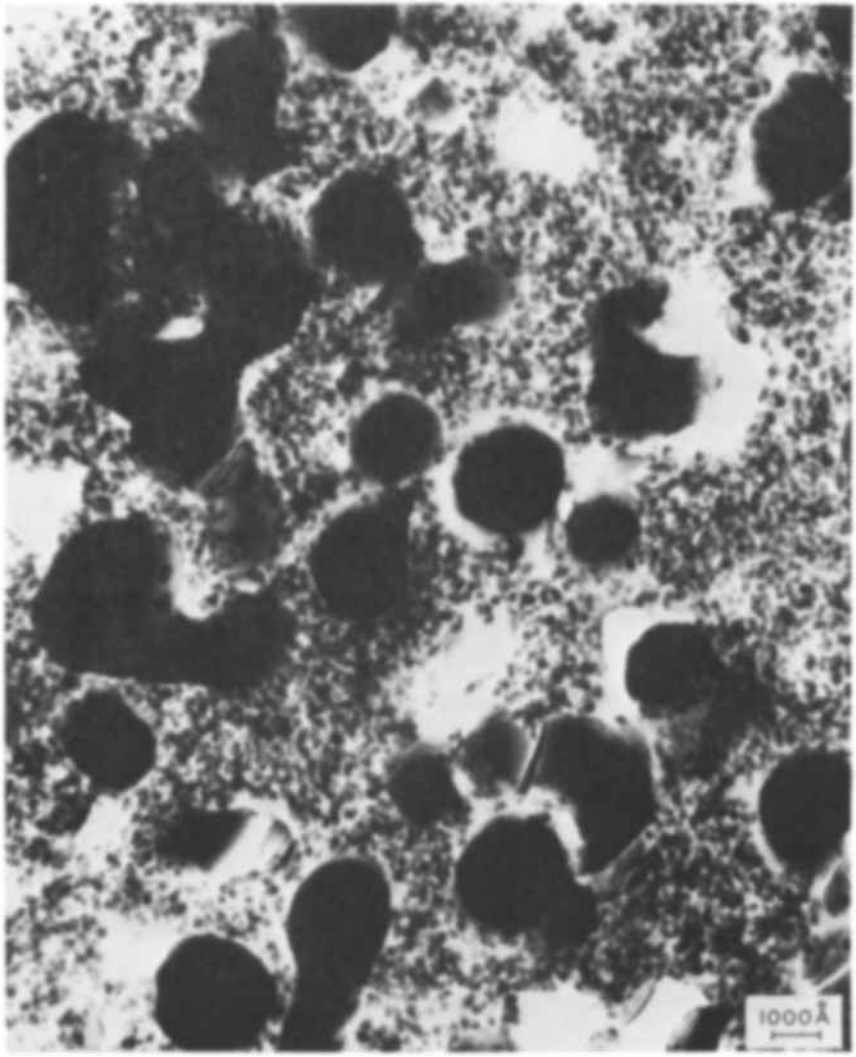

FIG. 3. Electron micrograph of broad pore diameter distribution Bio-Glas.

The field of Fig. 2 shows a group of open very large pores. In the same chip some of the smallest pores were noted. The pore diameters, measured on the perpendicular to a given dark surface (glass wall), range from 7500 to 250 Å. The average pore diameter was 3000 Å. All pores are very irregular. Materials with this large pore diameter were not seen in the previous study (*3*).

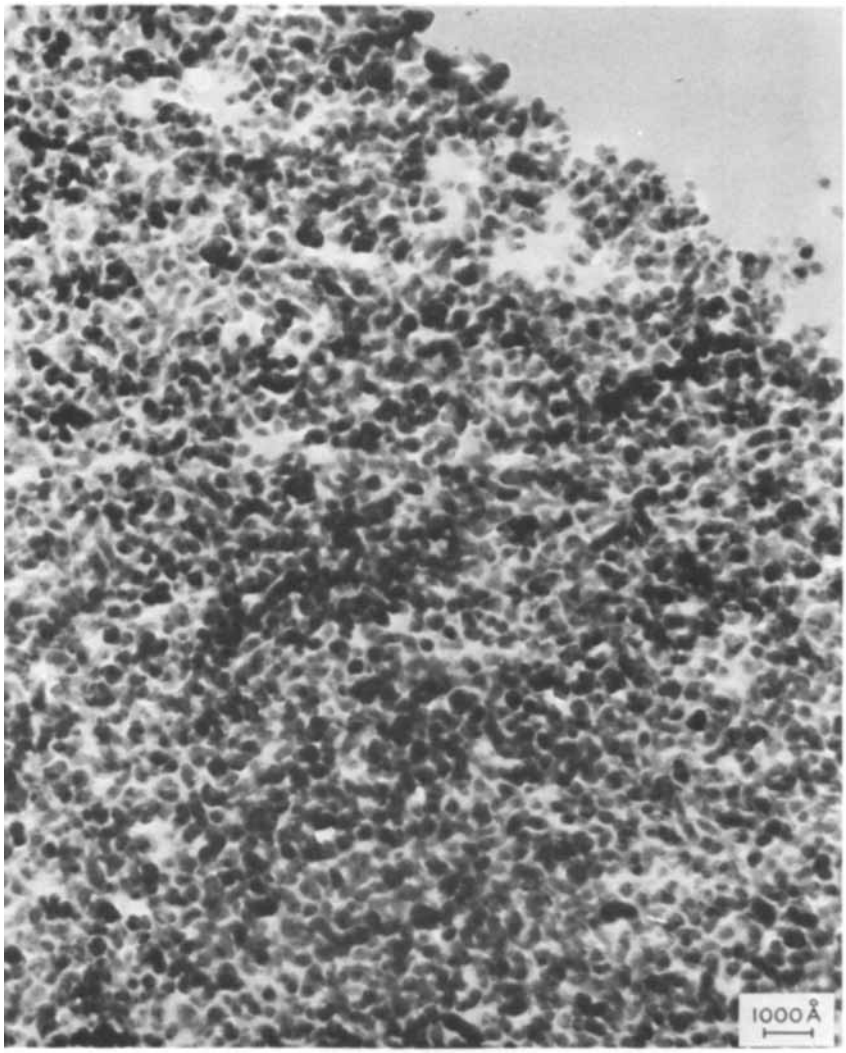

FIG. 4. Electron micrograph of broad pore diameter distribution Bio-Glas.

The field of Fig. 3 shows a material of about 100 Å pore diameter (granulations) which fills a structure similar to Fig. 2. This field was very near that shown in Fig. 2. The large, black voids represent the walls of the large matrix.

The relatively uniform field of Fig. 4 was taken at the edge of a chip. The average pore diameter is 200 Å with some large voids (filled with epoxy which precludes drop out) of 800 to 2000 Å diameter. Large

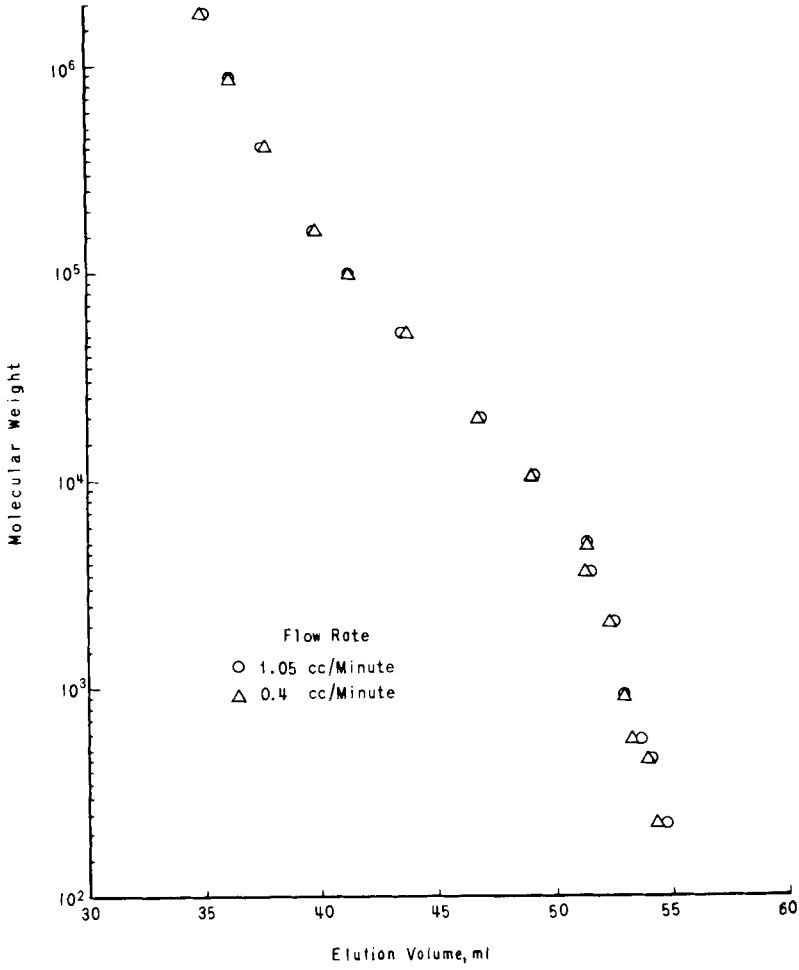

FIG. 5. Elution volume–molecular weight relationships for broad pore size distribution porous glass.

glass walls are notably absent near the edges of about half of the chips scanned.

The broad pore diameter distribution glass is a polydisperse material, not a mixture of various pore diameter chips. This is very clear in Fig. 3. Although it is not the purpose of this study to determine how this porous glass was made, the impression gained from Figs. 2–4 is

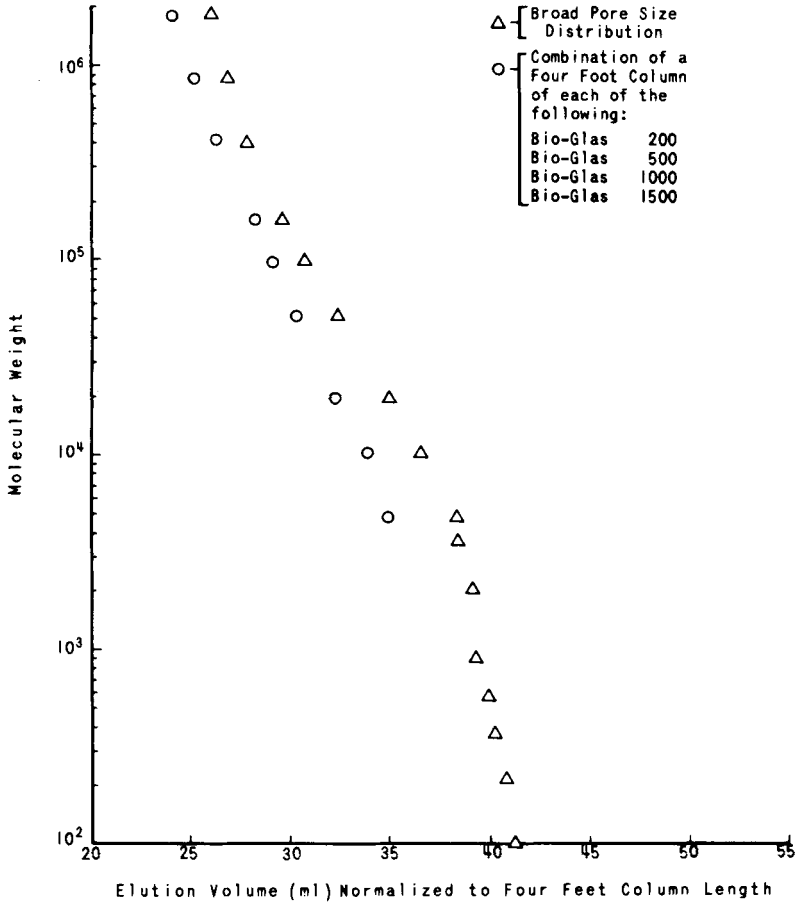

FIG. 6. Comparison of the elution volume–molecular weight relationships of the broad pore. Size distribution porous glass with a combination of narrower pore range porous glasses.

that a previously formed large pore diameter glass has been partially filled with a smaller pore diameter-forming glass. The effect is a product that appears to have undergone a series of treatments. Each chip contains a large number of microvolumes of differing pore sizes. If a broad pore size distribution substrate, mixed very intimately, has any real advantages in GPC, the Bio-Glas packing should exhibit the advantages fully.

GEL PERMEATION CHROMATOGRAPHY

The relationships between the elution volumes and the logarithm of the molecular weights of the polystyrene solutes at flow rates of 1.0 and 0.4 ml/min are shown in Fig. 5. The relationship exihibits the sigmoidal shape found for the other Bio-Glas substrates examined previously (*1*, *2*). The comparison between this column and four columns in series of varying but narrower pore size distribution Bio-Glas substrates, both normalized to 4-ft column length, is shown in Fig. 6. The curves are very similar in shape, the broad distribution column has a slightly flatter slope in the intermediate molecular weight region $0.5 \times 10^3 \rightarrow 1 \times 10^5$, and this exhibits greater selectivity with respect to the separation of the peak maxima of different molecular weights. This does not necessarily mean the column of broad pore size glass is more efficient, as this depends on the peak broadening also.

The elution volumes, peak widths, and the number of theoretical plates per foot for the polystyrene and hydrocarbon solutes at two different flow rates are recorded in Table 2. The column shows very little selectivity below molecular weights of 4000. Up to the highest molecular weights studied of 1.8×10^6 there is no flow rate dependence of elution volume for the flow rates studied. The number of theoretical plates, n, was calculated from the following equations:

$$n = \frac{1}{L}\left(\frac{V_e}{W_b/4}\right)^2 = \frac{1}{L}\left(\frac{V_e}{W_h/2.354}\right)^2 \qquad (1)$$

where V_e is the elution volume to the peak maximum, W_b is the peak width at the base, and W_h is the peak width at half the peak height.

The variation in the peak widths with molecular weight at both flow rates studied shows an initial increase with molecular weight up to 20,000, then a decrease. The number of theoretical plates calculated from Eq. (1) is dominated by the elution volume, V_e; and the values decrease regularly with increasing molecular weight except for molecular weights greater than 160,000 at the faster flow rate where a fairly constant value is found. The column performs more efficiently at the slower flow rate, and the increase in the number of theoretical plates is due to a decrease in the peak width since the elution volumes are constant. At molecular weights above 860,000, it appears that no increase in efficiency is obtained by slowing the flow rate from 1.05 to 0.4 ml/min. This is quite different from the results obtained with the 860,000 molecular weight polystyrene eluting from a polystyrene gel

TABLE 2

Elution Volumes, Peak Widths, and the Number of Theoretical Plates of Polystyrene Solutes Eluted from a Broad Pore Size Distribution Porous Glass Column at Two Flow Rates

	Flow rate									
	1.05 ml/min					0.4 ml/min				
		Peak width (ml)		Number of theoretical plates per foot, n, measured at			Peak width (ml)		Number of theoretical plates per foot, n, measured at	
Solutes	Elution volume (ml)	At the base, W_b	At half the peak height, W_h	The base	The peak half height	Elution volume (ml)	At the base, W_b	At half the peak height, W_h	The base	The peak half height
$nC_{16}H_{34}$	54.69	8.40	4.99	126.1	123.6	54.37	7.85	4.62	145.0	145.2
$nC_{24}H_{50}$	53.97	8.60	5.08	117.6	116.5	53.91	8.18	4.74	131.1	135.1
$nC_{40}H_{82}$	53.66	9.77	5.71	91	92.2	53.24	8.77	5.16	111.3	111.3
Polystyrene, $\bar{M}_w$										
900	52.83	9.82	5.72	86.1	88.1	52.82	8.94	5.03	105.5	115.1
2,030	52.49	10.03	5.80	81.5	84.4	52.36	9.03	5.24	101.8	104.2
3,600	51.52	10.50	6.09	71.7	73.6	51.31	9.11	5.37	95.9	95.5
4,800	51.43	10.16	5.84	76.3	79.9	51.42	9.09	5.26	98.2	100.6
10,300	49.10	10.50	6.05	65.1	67.8	49.04	9.45	5.57	81.6	80.9
19,800	46.94	10.29	5.97	62.0	63.8	46.81	9.45	5.50	74.4	76.0
51,000	43.47	9.61	5.63	60.9	61.4	43.76	9.03	5.33	71.3	70.7
97,200	41.23	9.53	5.55	55.8	56.9	41.36	8.65	5.08	69.4	69.7
160,000	39.79	9.61	5.51	51.0	53.9	39.85	8.52	4.95	66.4	68.0
411,000	37.59	9.40	5.38	47.6	50.4	37.70	8.52	4.91	59.5	62.0
860,000	36.22	8.76	5.08	52.0	53.6	36.20	8.81	5.04	51.3	54.4
1.8×10^6	35.11	8.76	5.08	48.9	50.4	35.06	9.17	5.33	45.1	45.6

column (*10*). There it was found that an increase in the number of theoretical plates per foot from 46 to 63 resulted from a similar change in flow rate. Moreover, it is interesting to note that the efficiency of the porous glass column is identical to that of the polystyrene gel column at this molecular weight.

The peak widths are largest for the samples that elute where the elution volume molecular weight relationship exhibits its smallest slope. This suggests that the discrete molecular weight range of the polystyrene samples may be influencing the total peak width. Assuming that the squares of the variances of the various processes occurring in the column are additive, the following equation may be written

$$W_{\text{total}}^2 = W_{\text{inst}}^2 + W_{\text{MWD}}^2 + W_{\text{GPC}}^2 \tag{2}$$

where W_{total}, W_{inst}, W_{MWD}, and W_{GPC} represent the widths of the peak due to the total process, the instrumental broadening, the molecular weight distribution, and the gel permeation chromatographic process, respectively. The latter consists of several parts which can be divided into two groups, those processes occurring within the pores and those occurring in the interstitial volume. The contributions W_{total} and W_{inst} were measured directly, the contributions from W_{MWD} were calculated assuming a log normal molecular weight distribution and using the calibration curve to determine the volumes between which molecular weights corresponding to 5 and 95% weight composition of a particular sample would elute.

The values of the peak widths W_{GPC} corrected for instrumental broadening and sample molecular weight inhomogeneity at each flow rate are collected in Table 3. Also included in this table are values of the number of theoretical plates n_{CHR} resulting only from the chromatographic process and calculated from the equation:

$$n_{\text{CHR}} = \frac{1}{L}\left(\frac{V_e - 3}{W_{\text{GPC}}/4}\right)^2 \tag{3}$$

The value of V_e is decreased by 3 ml, this being the holdup in the connecting tubings.

When the peak widths are corrected in this way, the values decrease fairly regularly with increasing molecular weight. This indicates that the efficiency of the separation process is not dependent upon the molecular diffusion coefficient as previously proposed (*11–13*).

TABLE 3

Correction of Experimental Peak Widths and Efficiencies for Instrumental Broadening and Sample Molecular Weight Inhomogeneity

Solute		W_{inst}^2 (ml²)	W_{MWD}^2 (ml²)	Flow rate: 1.05 ml/min W_{GPC}^2 (ml²)	Flow rate: 1.05 ml/min Number of theoretical plates/ft (n_{CHR})	Flow rate: 0.4 ml/min W_{GPC}^2 (ml²)	Flow rate: 0.4 ml/min Number of theoretical plates/ft (n_{CHR})
$C_{40}H_{82}$		7.8	0	87.7	87.2	69.1	110.7
Polystyrene $\bar{M}_w$	$\bar{M}_w/\bar{M}_n$						
10,300	1.06	10.9	6.8	92.6	68.4	71.6	88.4
19,800	1.06	10.9	7.3	87.7	65.6	71.1	80.9
51,000	1.06	10.9	7.8	73.7	66.2	62.8	77.7
97,200	1.06	11.6	6.8	72.4	60.2	56.4	77.3
160,000	1.06	11.6	5.3	75.5	53.4	55.7	72.4
411,000	1.06	11.6	2.0	74.8	47.6	59.0	60.4
860,000	1.15	11.6	1.4	63.7	51.6	64.6	50.9
860,000	1.72[a]	11.6	2.3	62.8	52.4	63.7	51.6

[a] Value based on a membrane osmometer determination of the number-average molecular weight = 500,000 obtained in this laboratory.

CONCLUSION

The porous glass substrate was shown to be a truly polydisperse pore size material and not a mixture of glasses with smaller pore size distributions. The material has been shown to be an effective substrate for the separation of macromolecules. The efficiency of the porous glass column used was as good as that of a polystyrene gel column at molecular weights near to 1 million, but the efficiency of the porous glass column was inferior at lower molecular weights. It appears there is no particular preference between using a broad pore size distribution packing material in gel permeation chromatography or a mixture of different but narrower pore size distribution materials.

Acknowledgment

A portion of the work of one author was supported by National Science Foundation Grant GP14440.

REFERENCES

1. M. J. R. Cantow and J. F. Johnson, *J. Appl. Polym. Sci.*, **11**, 1851 (1967).
2. M. J. R. Cantow and J. F. Johnson, *J. Polym. Sci., Part A-1*, **5**, 2835 (1967).
3. E. M. Barrall and J. H. Cain, *J. Polym. Sci., Part C*, **21**, 253 (1968).
4. W. Haller, *Nature*, **206**, 693 (1965).
5. J. C. Moore and M. C. Arrington, *Intern. Symp. Macromol. Chem., Tokyo, 1966*, pp. vi–107.
6. K. H. Altgelt and J. C. Moore, *Polymer Fractionation* (M. J. R. Cantow, ed.), Academic, New York, 1967.
7. A. R. Cooper and J. F. Johnson, *J. Appl. Polym. Sci.*, **13**, 1487 (1969).
8. D. O. Gray, *J. Chromatogr.*, **37**, 320 (1968).
9. W. W. Yau, M. L. Suchan, and C. P. Malone, *J. Polym. Sci., Part A-2*, **6**, 1349 (1968).
10. A. R. Cooper, A. R. Bruzzone, and J. F. Johnson, *Polym. Preprints*, **10**, 1455 (1969).
11. M. LePage and A. J. DeVries, *Third International Seminar on Gel Permeation Chromatography*, Geneva, Switzerland, 1966.
12. W. B. Smith and A. Kollmansberger, *J. Phys. Chem.*, **69**, 1457 (1965).
13. J. G. Hendrickson, *J. Polym. Sci., Part A-2*, **6**, 1903 (1968).

Received by editor October 16, 1969